Hindawi
International Journal of Antennas and Propagation
Volume 2022, Article ID 4046706, 13 pages
https://doi.org/10.1155/2022/4046706

*Research Article*

# Optimum Design of Multi-Section Asymmetrical Transdirectional Couplers with Port Impedance Matching up to S Band Frequency

**Homayoon Oraizi and Mohammad Javad Siahkari**

*School of Electrical Engineering, Iran University of Science and Technology, Tehran, Iran*

Correspondence should be addressed to Mohammad Javad Siahkari; m.j.siahkari@gmail.com

Received 28 December 2021; Revised 23 April 2022; Accepted 4 May 2022; Published 2 June 2022

Academic Editor: Chien-Jen Wang



The method of least squares is developed for the optimum design of multi-section asymmetrical transdirectional (ATRD) couplers with arbitrary port impedance matching. Firstly, transmission matrix of a section of coupler is obtained, then the transmission matrix of whole multi-section coupler is determined, from which the scattering matrix of device is obtained. An error function is then constructed by scattering parameters. According to design specifications, error function depends on physical parameters of coupler (such as widths, spacings and lengths of transmission line sections and capacitor values), of which minimum point gives optimum values of it's dimensions and capacitors. Optimum design is carried out for a specified frequency response and bandwidth. Error minimization is implemented by the combination of genetic algorithm (GA) and conjugate gradient method (CGM). The design is verified by full-wave simulation software, fabrication and measurement. Several 3 dB, 6 dB and 10 dB couplers are designed with different bandwidths and port impedances. Compared to the proposed design method, design of asymmetrical multi-section couplers by full-wave simulation softwares is by trial and error and at best random and almost impossible because of extremely high CPU time due to the large number of parameters of coupler geometrical structure.

## 1. Introduction

The directional couplers as passive microwave devices have extensive applications in RF designs, such as filters, phase shifters and measurement equipments. Its various types have been developed in different structures and platforms in the form of single and multi-section configurations [1–4]. The directional coupler is called as codirectional, contradirectional and transdirectional according to the placement of the isolated ports designated by 2, 3 and 4 as shown in Figure 1, respectively. Their use in the Butler matrix, leads to a complex configuration due to the crossover of circuit and parasitic effects [5]. For the remedy of this problem, the transdirectional coupler with capacitance loading is used in [6]. A characteristic of transdirectional (TRD) coupler is the achievement of specified coupling, with shorter lengths [7] and blocking of DC current to the through and coupled port. The last property, may be used in circuits where AC and DC signals exist together, such as active ones.

The design of symmetrical 3-section TRD coupler with 3 dB coupling and capacitance loading is presented in [6]. Each section of the structure is assumed as two directional coupler and analyzed by the even- and odd-mode theory. Due to the symmetry of structure, all attributes and properties of sections are identical. Inductance loadings in [7] are used for the miniaturization of symmetrical 3 dB TRD coupler. In this design, the coupler properties are the same as conventional ones, but the size has been reduced by about 50%. Since the realization of weak coupling is difficult in the symmetrical microstrip structures, the design of symmetrical TRD couplers with 10 dB and 20 dB coupling are carried out in CPW structures using DGS, capacitance loading and series inductances in [8]. A structure has been described in [8], consisting of three identical symmetrical sections. A more complex configuration is presented in [9], which uses compact capacitors, inductors and varactor diodes with DC bias to achieve arbitrary couplings for TRD coupler design. The variation of bias voltage of varactor

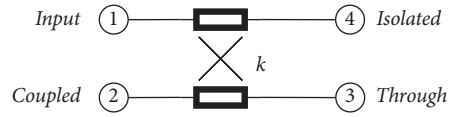


Figure 1: Schematic of transdirectional coupler.

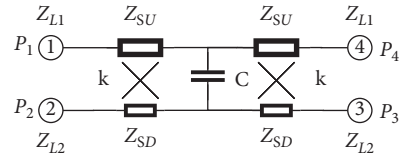


Figure 2: Structure of a section of transdirectional coupler with shunt capacitor loading.

diodes causes changing its capacitance value, which is used to change the coupling coefficient of symmetrical TRD coupler. With this configuration, 3–40 dB coupling coefficients has been achieved.

Various asymmetrical directional couplers and their design parameters are presented in [10–15]. The symmetrical directional coupler is generally used in practice which is analyzed by the even- and odd-mode theory. However, its parameters may be derived and specialized from the parameters of asymmetric directional coupler as a special case, as described in [15].

The microstrip asymmetric directional coupler can also be used as an impedance transformer. In [16], a 3 dB microstrip asymmetric directional coupler has been designed to behave as an impedance transformer from 50 ohm to 12.5 ohm in a power splitter for power amplifiers.

All the transdirectional couplers considered and reported in the literature, are designed based on symmetric structures employing coupled-line couplers and the even- and odd-mode analysis. Such methods are useful only for symmetric structures. However, for the design of asymmetric coupled lines with arbitrary port impedances incorporating impedance transformation, without any additional devices such as impedance matching networks, asymmetric multi-section structures should be used and analyzed by the methods based on $c$ and $\pi$ mode parameters.

In this paper, TRD couplers with port impedance matching are designed by the asymmetric transdirectional (ATRD) couplers with capacitance loading. The circuit model of ATRD coupler based on the asymmetric structure of coupled lines is analyzed and designed by the $c$ and $\pi$ modes using the four port network. This general model may be used for all the symmetrical and asymmetrical structures of coupled line TRD couplers. In addition to the symmetric transdirectional coupler properties and applications, this general asymmetric transdirectional coupler can also be used as impedance transformers in microwave designs. The single- and multi-section asymmetrical coupled-line couplers modeled as four port networks may be analyzed and designed.

The structure of a single section ATRD coupler with shunt capacitor loading is depicted in Figure 2, which is used as the base of ATRD coupler in this paper. Since the proposed structure consists of two asymmetric coupled lines and shunt capacitor, at first, the transmission matrix of an asymmetrical coupled-line and capacitor is obtained as a four port network. Then, the transmission matrix of the complete multi-section coupler structure and its scattering matrix are obtained. An error function is then constructed from the scattering parameters, according to the specified powers delivered to the ports of ATRD coupler. The frequency bandwidth and port impedances are also arbitrarily specified.

The five parameters of each section of ATRD coupler (widths of upper and lower strips, spacing between the two strips, length of the coupled lines and the value of shunt capacitor) and the relations among them (such as difference between the width of adjacent coupled line strips and spacings between two adjacent strips in a coupled line section, ranges and their relative values) should be consider in optimization. Without imposition of appropriate constraints on their values, an optimum design will not be obtained and there will appear fabrication and measurement problems. The design of microwave devices by merely using the commercial full-wave simulation softwares requires extensive CPU times. This situation is exacerbated in cases where the number of parameters is large. Usually the full-wave simulation softwares need initial values of parameters to start the optimization algorithms, on the other hand, the proposed design method in this paper based on the equivalent circuit model determines the optimum values of variables, by combining the global (GA) and local (CGM) optimization methods, irrespective of defining any initial value for each variable. Consequently, the extraction of appropriate equivalent circuits for ATRD coupler and the derivation of appropriate algorithms based on its required physical characteristics and specifications could effectively simplify and speed up the design process. The average CPU time of computer programs for each run of the presented devices in personal computer Core i5 @1.8 GHz, is about 80 times faster than the simulation with HFSS software in that computer. Since the used computer programs have high accuracy, the optimum design of devices by the presented method is significantly faster than the commercial full-wave simulation softwares.

An error function based on the method of least square (MLS) is constructed by scattering parameters of the equivalent circuit of ATRD according to the design specification. Its minimum point is then obtained by the combination of the genetic algorithm (GA) and conjugate gradient method (CGM). At first, GA searches for the convex space around the global minimum without specified initial value. Next, CGM use values has been obtained from GA as an initial value of optimization and searches rapidly for the global minimum point in the convex space. Such an algorithm combining GA and CGM determines the minimum point of error function realizing the design specifications and the optimum values of coupler parameters. The designed ATRD coupler is then simulated on the commercial full-wave softwares to obtain its frequency response to verify the MLS design. Several ATRD couplers are designed, fabricated and measured as proof of concept, to verify this method.

## 2. Design of Asymmetrical Transdirctional Coupler

The schematic diagram of an ATRD coupler loaded with shunt capacitor is depicted in Figure 2, which is composed of two coupled line sections and one intervening shunt capacitor. The input power (as $P_1$) at port (1) goes to the coupled port (2) (as $P_2$), goes directly to through port (3) (as $P_3$) but a small amount goes to isolated port (4) (as $P_4$). The characteristics of ATRD coupler are defined as coupling (C), directivity (D) and isolation (I).

According to physical and electrical characteristics of directional couplers, they are divided into symmetrical and asymmetrical structures. The symmetrical couplers may be analyzed by the even- and odd-mode method. Asymmetrical ones have more applications in the design of filters and impedance matching devices, which are designed by the $c$ and $\pi$ modes method.

A section of ATRD coupler as depict in Figure 2, is composed of two coupled lines with characteristic impedances $Z_{SU}$ and $Z_{SD}$ with different load impedances $Z_{L1}$ and $Z_{L2}$. Due to the different characteristics impedance of the upper and lower strip lines, they have different widths. Observe in Figure 2 that the proposed ATRD coupler consists of two identical asymmetrical directional couplers and a shunt capacitor, where $Z_{SU}$ and $Z_{SD}$ are the characteristic impedances of upper and lower lines of coupled lines, respectively, $k$ is the coupling coefficient of each coupled line, is the shunt capacitor placed between the two asymmetrical directional coupler, $Z_{L1}$ and $Z_{L2}$ are load impedance of upper and lower section of coupled line, respectively. Note that these coupled lines are identical. Because of the equal widths of two upper and lower sections in two adjacent directional couplers, the load impedances in upper and lower strips in left and right hand sides of structure are equal.

Since the device is a multifunction coupler combining coupling and impedance matching in a desired bandwidth, a multi-section structure should be employed, such as Figure 2. First, its whole transmission matrix should be extracted, by multiplying the transmission matrices of the coupled line and shunt capacitor as four port blocks.

Figure 3 depict an asymmetrical directional coupler, voltage and currents are assumed on each line. $(V_1, I_1)$, $(V_2, I_2)$, $(V_3, I_3)$ and $(V_4, I_4)$ are voltage and current pair ports 1,2,3 and 4, respectively. Now the normal mode parameters and impedance matrix of the coupled line in Figure 3 maybe obtained as described in [15]. In next step, the transmission matrix should be obtained from this impedance matrix. At first, this method can be developed to obtain the transmission matrix from impedance matrix for the four port network model of this structure.

Figure 4 depicts the block diagram with appropriate directions of current and voltages at its terminals for the [Z] matrix and similarly for [T].

Now the transmission matrix is derived from impedance matrix as a four port block, namely:

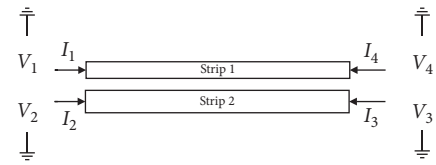


Figure 3: Structure of asymmetric directional coupler.

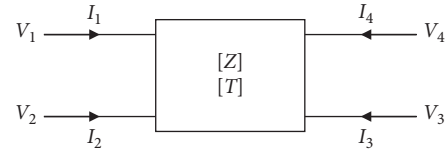


Figure 4: Schematic of current and voltage flow graph for asymmetrical directional coupler.

$$\begin{bmatrix} V_1 \\ V_2 \\ V_3 \\ V_4 \end{bmatrix} = \begin{bmatrix} \begin{bmatrix} Z_{11} & Z_{12} \\ Z_{21} & Z_{22} \end{bmatrix} & \begin{bmatrix} Z_{13} & Z_{14} \\ Z_{23} & Z_{24} \end{bmatrix} \\ \begin{bmatrix} Z_{31} & Z_{32} \\ Z_{41} & Z_{42} \end{bmatrix} & \begin{bmatrix} Z_{33} & Z_{34} \\ Z_{43} & Z_{44} \end{bmatrix} \end{bmatrix} \begin{bmatrix} I_1 \\ I_2 \\ I_3 \\ I_4 \end{bmatrix} = \begin{bmatrix} [Z_A] & [Z_B] \\ [Z_C] & [Z_D] \end{bmatrix} \begin{bmatrix} I_1 \\ I_2 \\ I_3 \\ I_4 \end{bmatrix}, \tag{1}$$

Equation (1) may be written as a four port transmission matrix:

$$\begin{bmatrix} V_1 \\ V_2 \\ I_1 \\ I_2 \end{bmatrix} = \begin{bmatrix} [Z_A][Z_C]^{-1} & [Z_B] - [Z_A][Z_C]^{-1}[Z_D] \\ [Z_C]^{-1} & -[Z_C]^{-1}[Z_D] \end{bmatrix} \begin{bmatrix} V_3 \\ V_4 \\ I_3 \\ I_4 \end{bmatrix} = \begin{bmatrix} \begin{bmatrix} T_{11} & T_{12} \\ T_{21} & T_{22} \end{bmatrix} & \begin{bmatrix} T_{13} & T_{14} \\ T_{23} & T_{24} \end{bmatrix} \\ \begin{bmatrix} T_{31} & T_{32} \\ T_{41} & T_{42} \end{bmatrix} & \begin{bmatrix} T_{33} & T_{34} \\ T_{43} & T_{44} \end{bmatrix} \end{bmatrix} \begin{bmatrix} V_3 \\ V_4 \\ I_3 \\ I_4 \end{bmatrix}. \tag{2}$$

The directions of currents at ports 3 and 4 for transmission matrix are defined opposite to those of impedance matrix as indicated in Figure 4. Therefore, (3) may be written for the transmission matrix of four port network as follows:

$$\begin{bmatrix} V_1 \\ V_2 \\ I_1 \\ I_2 \end{bmatrix} = \begin{bmatrix} \begin{bmatrix} T_{12} & T_{11} \\ T_{22} & T_{21} \end{bmatrix} & \begin{bmatrix} -T_{14} & -T_{13} \\ -T_{24} & -T_{23} \end{bmatrix} \\ \begin{bmatrix} T_{32} & T_{31} \\ T_{42} & T_{41} \end{bmatrix} & \begin{bmatrix} -T_{34} & -T_{33} \\ -T_{44} & -T_{43} \end{bmatrix} \end{bmatrix} \begin{bmatrix} V_4 \\ V_3 \\ -I_4 \\ -I_3 \end{bmatrix} = \underbrace{\begin{bmatrix} [A] & [B] \\ [C] & [D] \end{bmatrix}}_{[T_{\text{Coupled}}]} \begin{bmatrix} V_4 \\ V_3 \\ -I_4 \\ -I_3 \end{bmatrix}. \tag{3}$$

Compared to (2), the columns of submatrices $[Z_A][Z_C]^{-1}$, $[Z_C]^{-1}$ are interchanged and columns of submatrices $[Z_B] - [Z_A][Z_C]^{-1}[Z_D]$ and $-[Z_C]^{-1}[Z_D]$ are interchanged and are also multiplied by the negative sign. From (3) the impedance matrix of asymmetrical directional coupler as in [15] can be transformed to the transmission matrix, called $[T_{\text{Coupled}}]$.

The transmission matrix of shunt capacitor as a four port block shown in Figure 5 is then obtained. The voltage relations are $V_1 = V_4$ and $V_2 = V_3$. The outward currents of ports 4 and 3 are defined as $-I_4$ and $-I_3$, respectively. Therefore:

$$I_1 - Y(V_1 - V_2) + I_4 = 0, \quad I_2 + Y(V_1 - V_2) + I_3 = 0, \quad (4)$$

The transmission matrix of the four port network of capacitor is denoted as $[T_{\text{Cap}}]$:

$$\begin{bmatrix} V_1 \\ V_2 \\ I_1 \\ I_2 \end{bmatrix} = \underbrace{\begin{bmatrix} 1 & 0 & 0 & 0 \\ 0 & 1 & 0 & 0 \\ Y & -Y & 1 & 0 \\ -Y & Y & 0 & 1 \end{bmatrix}}_{[T_{\text{Cap}}]} \begin{bmatrix} V_4 \\ V_3 \\ -I_4 \\ -I_3 \end{bmatrix}, \quad (5)$$

Therefore the transmission matrix of a section of ATRD coupler as depicted in Figure 2, is obtain as $[T]$:

$$[T] = \left[T_{\text{Coupled}}\right]\left[T_{\text{Cap}}\right]\left[T_{\text{Coupled}}\right]. \quad (6)$$

Now the N-section asymmetrical transdirectional coupler composed of coupled-lines and shunt capacitors maybe drawn in Figure 6. It consists of N-sections of a ATRD coupler, as shown in Figure 2, and lead and load sections.

The termination loads are $Z_{L1}, Z_{L2}, Z_{L3}$ and $Z_{L4}$ at ports 1, 2, 3 and 4, respectively. Therefore, the specified coupled power as well as impedance matching has been realized.

For the design of ATRD coupler, its transmission matrix is first obtained as:

$$[T_{ATRD}] = \left\{ \prod_{i=1}^{N} \left[T_{\text{Coupled}}\right]_i \left[T_{\text{Cap}}\right]_i \left[T_{\text{Coupled}}\right]_i \right\}. \quad (7)$$

The complete ATRD coupler is shown in Figure 6, including the lead and load sections at its ports, with transmission matrices denoted as $[T_{\text{Lead}}]$ and $[T_{\text{Load}}]$, respectively. Their evaluations are described in [17]. The lead and load sections are shown in Figure 7, which are depict as

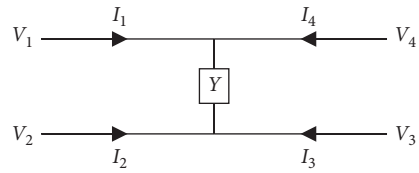


Figure 5: Schematic of shunt capacitance as four port block.

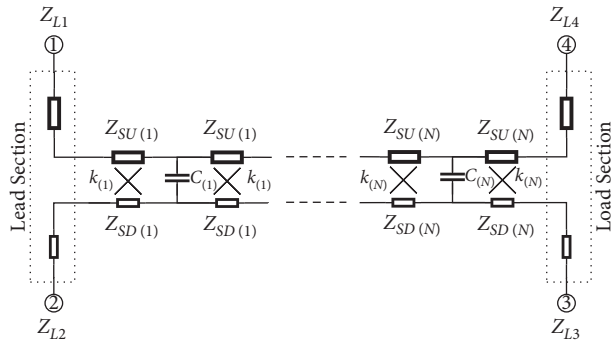


Figure 6: Schematic of multi section asymmetrical transdirectional coupler with capacitance shunt load.

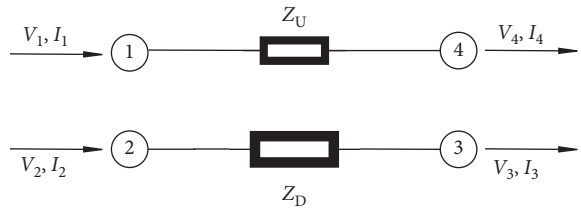


Figure 7: Schematic of lead/load sections.

transmission lines. Based on [17], it's transmission matrix is obtained as (8), where $\gamma_U$ and $\gamma_D$ are propagation constants of upper and lower transmission lines, $l_U$ and $l_D$ are lengths of upper and lower transmission lines, $Z_U$ and $Y_U$ are impedance and admittance of upper transmission line, $Z_D$ and $Y_D$ are impedance and admittance of lower transmission line, respectively. These transmission lines are used to connect SMA connectors to the main ATRD coupler. As its clear, for archive acceptable impedance matching in each port, the widths of transmission line of the lead or load lines should be equal to same section of ATRD coupler witch connected to it. Also to reduce the mismatch effect, the transmission lines have been connected to ATRD coupler by bends.

$$\begin{bmatrix} V_1 \\ V_2 \\ I_1 \\ I_2 \end{bmatrix} = \begin{bmatrix} \cosh(\gamma_U l_U) & 0 & Z_U \sinh(\gamma_U l_U) & 0 \\ 0 & \cosh(\gamma_D l_D) & 0 & Z_D \sinh(\gamma_D l_D) \\ Y_U \sinh(\gamma_U l_U) & 0 & \cosh(\gamma_U l_U) & 0 \\ 0 & Y_D \sinh(\gamma_D l_D) & 0 & \cosh(\gamma_D l_D) \end{bmatrix} \begin{bmatrix} V_3 \\ V_4 \\ I_3 \\ I_4 \end{bmatrix}, \tag{8}$$

$$\begin{aligned} \text{error} = \Bigg\{ & W_1 \sum_{m=1}^{M} \left|S_{11}\right|^2 + W_2 \sum_{m=1}^{M} \left|S_{22}\right|^2 + W_3 \sum_{m=1}^{M} \left|S_{33}\right|^2 + W_4 \sum_{m=1}^{M} \left|S_{44}\right|^2 + W_5 \sum_{m=1}^{M} \left|S_{14}\right|^2 +, \\ & W_6 \sum_{m=1}^{M} \left[\left|S_{12}\right| - C\right]^2 + W_7 \sum_{m=1}^{M} \left[\left|S_{13}\right| - T\right]^2 \Bigg\} + \cdots, \\ & \Bigg\{ W_8 \sum_{n=1}^{N} \left[\left|S_{12}^U\right| - L_C^U\right]^2 + W_9 \sum_{n=1}^{N} \left[\left|S_{12}^D\right| - L_C^D\right]^2 + W_{10} \sum_{n=1}^{N} \left[\left|S_{13}^U\right| - L_T^U\right]^2 + W_{11} \sum_{n=1}^{N} \left[\left|S_{13}^D\right| - L_T^D\right]^2 \Bigg\}. \end{aligned} \tag{9}$$

Therefore, considering the effect of lead and load sections in the design of ATRD coupler, the complete transmission matrix of ATRD coupler should be as:

$$\left[T_{\text{Coupler}}\right] = \left[T_{\text{Lead}}\right]\left[T_{ATRD}\right]\left[T_{\text{Load}}\right]. \tag{10}$$

where $[T_{\text{ATRD}}]$ is calculated in (7). Finally, The scattering matrix is defined as:

$$\begin{aligned} [S] &= \sqrt{[Y_{\text{Term}}]}\,[Z_M]\,[Z_P]\sqrt{[Z_{\text{Term}}]}, \\ [Z_M] &= \left[Z_{\text{Coupler}}\right] - [Z_{\text{Term}}], \\ [Z_P] &= \left[Z_{\text{Coupler}}\right] + [Z_{\text{Term}}]. \end{aligned} \tag{11}$$

where $[Z_{\text{Coupler}}]$ is the impedance matrix of the ATRD and $[Y_{\text{Term}}]$, $[Z_{\text{Term}}]$ are the diagonal admittance and impedance matrices of the termination loads. In order to calculate the scattering matrix of ATRD, the impedance matrix of the whole structure, $[Z_{\text{Coupler}}]$ in (11), should first be extracted from the transmission matrix, $[T_{\text{Coupler}}]$ in (10).

The transmission matrix of four port structure in (3) may be used to obtain the impedance matrix of the coupler:

$$\begin{bmatrix} V_1 \\ V_2 \\ V_4 \\ V_3 \end{bmatrix} = \begin{bmatrix} [A][C]^{-1} & -[A][C]^{-1}[D] + [B] \\ [C]^{-1} & -[C]^{-1}[D] \end{bmatrix} \begin{bmatrix} I_1 \\ I_2 \\ -I_4 \\ -I_3 \end{bmatrix}, \tag{12}$$

or,

$$\begin{bmatrix} V_1 \\ V_2 \\ V_3 \\ V_4 \end{bmatrix} = \begin{bmatrix} \begin{bmatrix} Z_{11} & Z_{12} \\ Z_{21} & Z_{22} \end{bmatrix} & \begin{bmatrix} Z_{13} & Z_{14} \\ Z_{23} & Z_{24} \end{bmatrix} \\ \begin{bmatrix} Z_{31} & Z_{32} \\ Z_{41} & Z_{42} \end{bmatrix} & \begin{bmatrix} Z_{33} & Z_{34} \\ Z_{43} & Z_{44} \end{bmatrix} \end{bmatrix} \begin{bmatrix} I_1 \\ I_2 \\ -I_4 \\ -I_3 \end{bmatrix}. \tag{13}$$

Which may be written into form of standard impedance equation:

$$\begin{aligned} \begin{bmatrix} V_1 \\ V^1 \\ V^2 \\ V_4^3 \end{bmatrix} &= \begin{bmatrix} \begin{bmatrix} Z_{11} & Z_{12} \\ Z^{21} & Z^{22} \\ Z_{41} & Z_{42} \\ Z_{31} & Z_{32} \end{bmatrix} & \begin{bmatrix} -Z_{14} & -Z_{13} \\ -Z^{24} & -Z^{23} \\ -Z_{44} & -Z_{43} \\ -Z_{34} & -Z_{33} \end{bmatrix} \end{bmatrix} \begin{bmatrix} I_1 \\ I^2 \\ I_3^3 \\ I_4 \end{bmatrix}, \\ &= \underbrace{\begin{bmatrix} \begin{bmatrix} Z_A \\ Z_C \end{bmatrix} & \begin{bmatrix} Z_B \\ Z_D \end{bmatrix} \end{bmatrix}}_{\left[Z_{\text{Coupler}}\right]} \begin{bmatrix} I_1 \\ I^2 \\ I_3^3 \\ I_4 \end{bmatrix}. \end{aligned} \tag{14}$$

The substitution of impedance matrix $[Z_{\text{Coupler}}]$ from into (14), (11) gives the scattering matrix of the asymmetrical four port network with different terminations. An error function is then constructed for the design of ATRD coupler as (8).

Where $C$ and $S_{12}$ are the desired and actual coupling coefficients at port (2), $T$ and $S_{13}$ are the desired and actual signals delivered to the through port (3), $S_{11}$, $S_{22}$, $S_{33}$ and $S_{44}$ are the reflection losses at ports 1, 2, 3 and 4, respectively, $S_{14}$ is the isolation between ports (1) and (4).

The desired frequency responses of coupled and through ports of the ATRD coupler are drawn in Figure 8. Observe that from $f_L$ to $f_H$ (in band), the power delivered to coupled and through ports is indicated as $C$ and $T$, respectively. The coupler should be designed in such a way that the expected power losses are realized in the bands from $f_D$ to lower frequencies (lower out band) and from $f_U$ to upper frequencies (upper out band).

The error function in (8) and (9), is constructed to satisfy the desired frequency response, where the in band from $f_L$ to $f_H$ is divided into $M$ discrete frequencies and the lower and upper out bands are each divided into N discrete frequencies. Also, $L_C^U$ and $L_C^D$ are the desired attenuations of the coupled port in the lower and upper out band and $S_{12}^U, S_{12}^D$ are the corresponding scattering parameters, respectively. The corresponding parameters for the through port are $L_T^U, L_T^D, S_{13}^U$ and $S_{13}^D$ $W_1$ to $W_{11}$ are weighting factors of each error term in (8) and (9). All of these parameters are assigned in the optimization process to achieve the desired frequency response.

The error values are obtained from the error function, which depends on the widths, lengths, spacings and capacitors of each section of the multi-section ATRD coupler. Its minimization gives the optimum values of its geometrical dimensions for the realization of its design specification. The minimization of the error function is performed by the combination of genetic algorithm(GA), which is a slow global minimum seeking algorithm and the fast conjugate gradient method (CGM) which is a local seeking algorithm. The minimization process starts by the **GA** which does not need the initial values of parameters and the process is then handed-over to **CGM** to finally locate the absolute minimum. It should be note that, at the end of optimization, capacitors are rounded to the nearest values of available standard

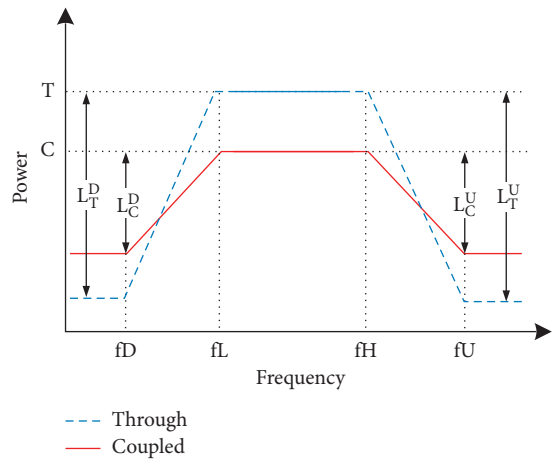


Figure 8: Frequency response of couple port and through port.

Table 1: Values of (9) for design 3 dB ATRD coupler has been described in Example 1.

| $W_1$ | $W_2$ | $W_3$ | $W_4$ | $W_5$ | $W_6$ | $W_7$ | $W_8$ | $W_9$ | $W_{10}$ | $W_{11}$ | $C$ $(dB)$ | $T$ $(dB)$ | $L_C^U$ $(dB)$ | $L_C^D$ $(dB)$ | $L_T^U$ $(dB)$ | $L_T^D$ $(dB)$ |
|---|---|---|---|---|---|---|---|---|---|---|---|---|---|---|---|---|
| 1 | 1 | 1 | 1 | 1 | 4 | 4 | 2 | 2 | 2 | 2 | −3 | −3 | −6 | −6 | −6 | −6 |

Table 2: Dimension and capacitor value for design 3 dB ATRD coupler has been described in Example 1.

| Section | $W_{U(i)}$ $(mm)$ | $W_{D(i)}$ $(mm)$ | $S_{(i)}$ $(mm)$ | $L_{(i)}$ $(mm)$ | $C_{(i)}$ $(pF)$ |
|---|---|---|---|---|---|
| 1 | 1.3 < **1.36** < 2 | 0.5 < **0.83** < 1 | 0.2 < **0.50** <2 | 0.5 < **0.70** < 4 | 0.2 < **0.25** < 4 |
| 2 | 0.2 < **0.47** < 2 | 0.2 < **0.99** < 2 | 0.2 < **0.93** < 2 | 0.5 < **0.96** < 4 | 0.2 < **1** < 4 |
| 3 | 0.2 < **0.40** < 2 | 0.2 < **1.36** < 2 | 0.2 < **0.59** < 2 | 0.5 < **0.76** < 4 | 0.2 < **0.25** < 4 |
| 4 | 0.2 < **0.40** < 2 | 0.2 < **1.11** < 2 | 0.2 < **0.50** < 2 | 0.5 < **1.59** < 4 | 0.2 < **0.25** < 4 |
| 5 | 0.2 < **0.40** < 2 | 0.2 < **0.70** < 2 | 0.2 < **0.52** < 2 | 0.5 < **0.74** < 4 | 0.2 < **0.5** < 4 |
| 6 | 0.2 < **0.40** < 2 | 0.2 < **0.42** < 2 | 0.2 < **0.50** < 2 | 0.5 < **0.70** < 4 | 0.2 < **0.25** < 4 |
| 7 | 0.2 < **0.40** < 2 | 0.2 < **0.40** < 2 | 0.2 < **0.50** < 2 | 0.5 < **1.31** < 4 | 0.2 < **1.2** < 4 |
| 8 | 0.2 < **0.41** < 2 | 0.2 < **0.60** < 2 | 0.2 < **0.58** < 2 | 0.5 < **1.42** < 4 | 0.2 < **2** < 4 |
| 9 | 0.2 < **0.45** < 2 | 0.2 < **0.82** < 2 | 0.2 < **0.96** < 2 | 0.5 < **1.29** < 4 | 0.2 < **0.25** < 4 |
| 10 | 1.3 < **1.35** < 2 | 1.3 < **1.98** < 2 | 0.2 < **0.50** < 2 | 0.5 < **0.71** < 4 | 0.2 < **3** < 4 |

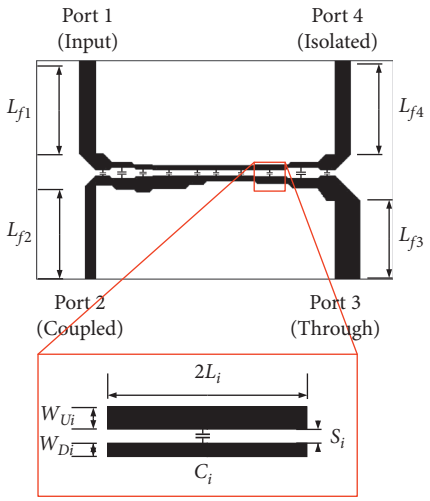


Figure 9: Schematic of 3 dB ATRD Coupler, has been described in Example 1.

Table 3: Dimension of feed lines for design 3 dB ATRD coupler has been described in Example 1.

| $L_{f1}$ $(mm)$ | $L_{f2}$ $(mm)$ | $L_{f3}$ $(mm)$ | $L_{f4}$ $(mm)$ |
|---|---|---|---|
| 25.6 | 25.6 | 24.3 | 25.6 |

capacitors. Then the final optimization algorithm that use these standard capacitors is carried out by **CGM**. To start the design and optimization, at first the parameters of (8) and (9) such as weight factors, desired frequency-band of coupler, insertion loss and out-of- band loss values are specified. Then, the acceptable range of variables are specified. After that, the minimization algorithms of **GA** and **CGM** are performed. Finally, minimum point of error is located and the geometrical dimensions of the ATRD coupler are determined.

## 3. Examples of Numerical Design, Fabrication and Measurement

For the validation of the proposed design method of ATRD coupler, three examples of ATRD couplers are presented

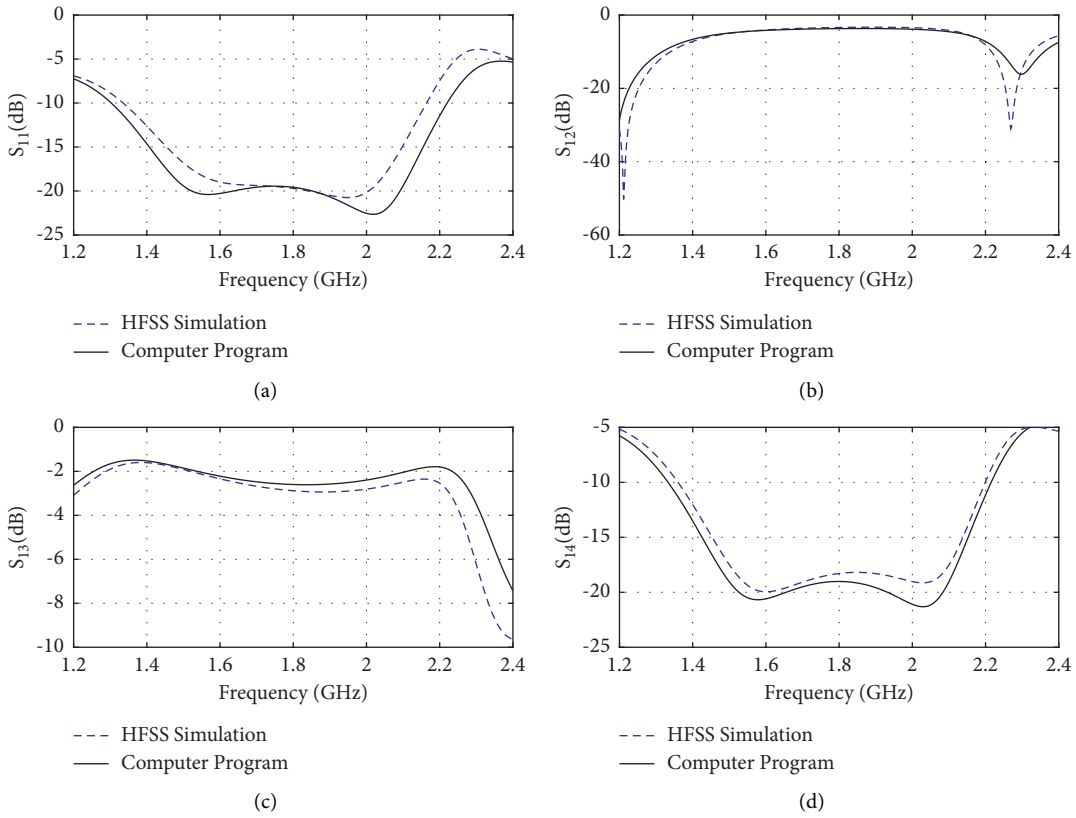


Figure 10: Frequency response of 3 dB ATRD coupler. (a) Reflection Loss; (b) Coupling coefficient; (c) Through coefficient; (d) Isolation coefficient.

with specified coupling coefficient of 3 dB, 6 dB and 10 dB. They are selected to check the effectiveness of method for weak and strong couplings with arbitrary port impedances, up to S band frequency. It should be noted that, the circuit model of ATRD coupler that based on asymmetric directional coupler, is valid over $X$ band frequency, but for fabrication limitation, such as PCB accuracy and available capacitors these examples are designed up to S band frequency.

The design process starts by assign the design specifications of coupling coefficients, port impedances, frequency bandwidth, number of sections and dielectric characteristics of substrate. Then, the acceptable range and bounds of relevant parameters of (8) and (9) are assigned. The final values of each parameter after the optimization are shown in bold between two bounds in each table, witch this bound is the acceptable variation range of variables in optimization process. All simulations (full-wave and computer program) are in personal computer Core i5 @1.8 GHz.

The scattering parameters of each ATRD coupler is illustrated and described in each example. The measurements have been done by Agilent E5071C. Since the port impedance of network analyzers is 50-ohm and the measured parameters are made on the basis of 50-ohm, in Sections 3.2 and 3.3 the measured values are converted to the specified impedances used in the design and optimization by the process has been described in detail in [18].

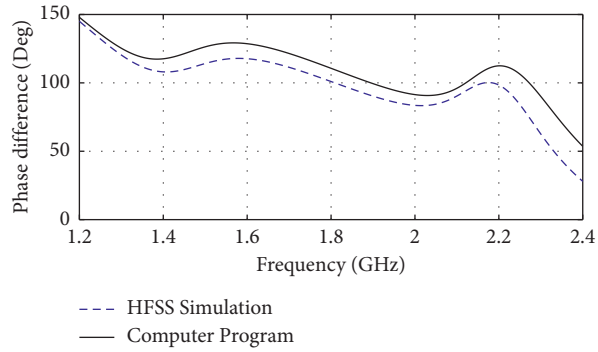


Figure 11: Phase difference between through and coupled ports of 3 dB ATRD coupler.

*3.1. Example 1: Design 3 dB Asymmetric Transdirectional Coupler.* A 3 dB ATRD coupler is designed with terminal impedances of 50, 75, 50 and 50 ohms at ports 1,2,3 and 4, respectively. It has been designed on 1.5–2.1 GHz, which allocated to the mobile frequency band. It is composed of 10 sections and designed on the Rogers 4003 substrate with dielectric constant $\varepsilon_r = 3.38$, $\tan(\delta) = 0.0027$ and thickness = 0.8 mm. The parameters of (8) and (9) are set as in Table 1 to design a 3 dB ATRD coupler with 6 dB out-of-band losses for through and coupled ports. The final values of dimensions and capacitors as well as their variation range in optimization process are shown in Table 2. Its schematic

Table 4: Values of (9) for design 6 dB ATRD coupler has been described in Example 2.

| $W_1$ | $W_2$ | $W_3$ | $W_4$ | $W_5$ | $W_6$ | $W_7$ | $W_8$ | $W_9$ | $W_{10}$ | $W_{11}$ | $C\ (dB)$ | $T\ (dB)$ | $L_C^U\ (dB)$ | $L_C^D\ (dB)$ | $L_T^U\ (dB)$ | $L_T^D\ (dB)$ |
|---|---|---|---|---|---|---|---|---|---|---|---|---|---|---|---|---|
| 1 | 1 | 1 | 1 | 1 | 4 | 4 | 2 | 2 | 2 | 2 | −6 | −1.25 | −9 | −9 | −4.5 | −4.5 |

Table 5: Dimension and capacitor value for design 6 dB ATRD coupler has been described in Example 2.

| Section | $W_U(i)\ (mm)$ | $W_D(i)\ (mm)$ | $S(i)\ (mm)$ | $L(i)\ (mm)$ | $C(i)\ (pF)$ |
|---|---|---|---|---|---|
| 1 | $1 < \mathbf{1.9} < 2$ | $0.9 < \mathbf{0.95} < 1.1$ | $0.2 < \mathbf{0.7} < 2$ | $0.5 < \mathbf{1.3} < 6$ | $0.2 < \mathbf{0.2} < 4$ |
| 2 | $0.2 < \mathbf{1.5} < 3$ | $0.2 < \mathbf{1.35} < 3$ | $0.2 < \mathbf{0.6} < 2$ | $0.5 < \mathbf{1.5} < 6$ | $0.2 < \mathbf{0.5} < 4$ |
| 3 | $0.2 < \mathbf{0.9} < 3$ | $0.2 < \mathbf{0.8} < 3$ | $0.2 < \mathbf{0.55} < 2$ | $0.5 < \mathbf{1.3} < 6$ | $0.2 < \mathbf{0.2} < 4$ |
| 4 | $0.2 < \mathbf{0.75} < 3$ | $0.2 < \mathbf{0.95} < 3$ | $0.2 < \mathbf{0.55} < 2$ | $0.5 < \mathbf{1.2} < 6$ | $0.2 < \mathbf{1} < 4$ |
| 5 | $0.2 < \mathbf{1.3} < 3$ | $0.2 < \mathbf{1.65} < 3$ | $0.2 < \mathbf{0.6} < 2$ | $0.5 < \mathbf{1.1} < 6$ | $0.2 < \mathbf{0.2} < 4$ |
| 6 | $0.2 < \mathbf{0.75} < 3$ | $0.2 < \mathbf{1.65} < 3$ | $0.2 < \mathbf{0.8} < 2$ | $0.5 < \mathbf{1.25} < 6$ | $0.2 < \mathbf{1} < 4$ |
| 7 | $0.2 < \mathbf{1.4} < 3$ | $0.2 < \mathbf{1.75} < 3$ | $0.2 < \mathbf{0.7} < 2$ | $0.5 < \mathbf{1.25} < 6$ | $0.2 < \mathbf{0.2} < 4$ |
| 8 | $0.2 < \mathbf{2} < 3$ | $0.2 < \mathbf{2} < 3$ | $0.2 < \mathbf{0.8} < 2$ | $0.5 < \mathbf{2.75} < 6$ | $0.2 < \mathbf{0.5} < 4$ |
| 9 | $0.2 < \mathbf{1.55} < 3$ | $0.2 < \mathbf{1} < 3$ | $0.2 < \mathbf{0.85} < 2$ | $0.5 < \mathbf{5.65} < 6$ | $0.2 < \mathbf{0.2} < 4$ |
| 10 | $1 < \mathbf{1.1} < 2$ | $0.6 < \mathbf{0.7} < 0.8$ | $0.2 < \mathbf{0.65} < 2$ | $0.5 < \mathbf{1.15} < 6$ | $0.2 < \mathbf{0.2} < 4$ |

Table 6: Dimension of feed lines for design 6 dB ATRD coupler has been described in Example 2.

| $L_{f1}\ (mm)$ | $L_{f2}\ (mm)$ | $L_{f3}\ (mm)$ | $L_{f4}\ (mm)$ |
|---|---|---|---|
| 6.1 | 6.1 | 6.4 | 7 |

diagram is shown in Figure 9. One section is drawn in a larger scale to show the dimensions clearly. The dimensions of the lead and load lines after optimization are given in Table 3. Because of the obtained spacings between coupled lines after optimization are smaller than the smallest available standard capacitor sizes (0402 in inch) and also because of the difficulties of assembly of smaller capacitors, this 3 dB coupler is not fabricated. Therefore, the results of computer program and full-wave software are provided merely to verify this method. Every loop of computer program optimization on personal computer Core i5 @1.8 GHz, takes **4.951707 seconds**. On the other hand, HFSS software takes **534 seconds** for this process. Therefore, computer program is about 107 times faster than the full-wave simulation software in this example.The frequency responses of the designed ATRD coupler as obtained by the full-wave computer software (HFSS) and by the equivalent circuit, are drawn in the figures. The full-wave simulation (HFSS) and equivalent circuit model (Computer program) results for the scattering parameters $S_{11}$, $S_{12}$, $S_{13}$ and $S_{14}$ are shown in Figures 10, 10(a)a–c10(c) and 10(d), respectively. Notice that HFSS simulation is a full-wave simulation that includes all of effective parameters of the structure. However, The design procedure based on the equivalent circuit is developed to speed up the design and optimization, which does account for some parameters, such as actual size of capacitors and exact mutual electromagnetic effect of sections and materials. However, the results of circuit model and full-wave electromagnetic model agree quite well. On the other hand, the final design of ATRD coupler is adjusted by the full-wave optimization. The −20 dB isolation bandwidth is 28.3% in the frequency bandwidth 1.53–2.04 GHz.

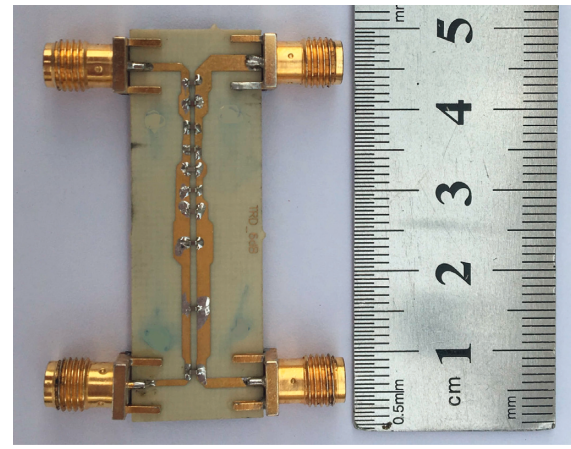


Figure 12: Fabricated 6 dB ATRD coupler of Example 2.

In this bandwidth the coupler coefficient is $3 \pm 1$ and through value is also $3 \pm 1$ dB. The phase difference between coupled and through port are shown in Figure 11. Results of computer program and HFSS simulation have good agreement. The HFSS phase difference is $100 \pm 15^{\circ}$ in 1.53–2.04 GHz frequency range.

*3.2. Example 2: Design 6 dB Asymmetric Transdirectional Coupler.* A 6 dB ATRD coupler is designed with different port impedance of 50, 70, 80 and 50 ohms at ports 1,2,3 and 4, respectively. It has been designed on 3.3–3.7 GHz, which allocated to the WI-MAX frequency band. It is composed of 10 sections and designed on the Rogers 4003 substrate with thickness = 0.8mm. The parameters of (8) and (9) are set as in Table 4 for design a 6 dB ATRD coupler. To achieve the 6 dB ATRD coupler, C sets to −6 dB, $T$ sets to −1.25 dB and attenuation in out of bands sets about 3 dB lower than C and $T$ values in coupled and through ports. The final values of dimensions and capacitors as well as their variation range in optimization process are shown in Table 5. The dimensions of terminal lines are given in Table 6. Every loop of computer

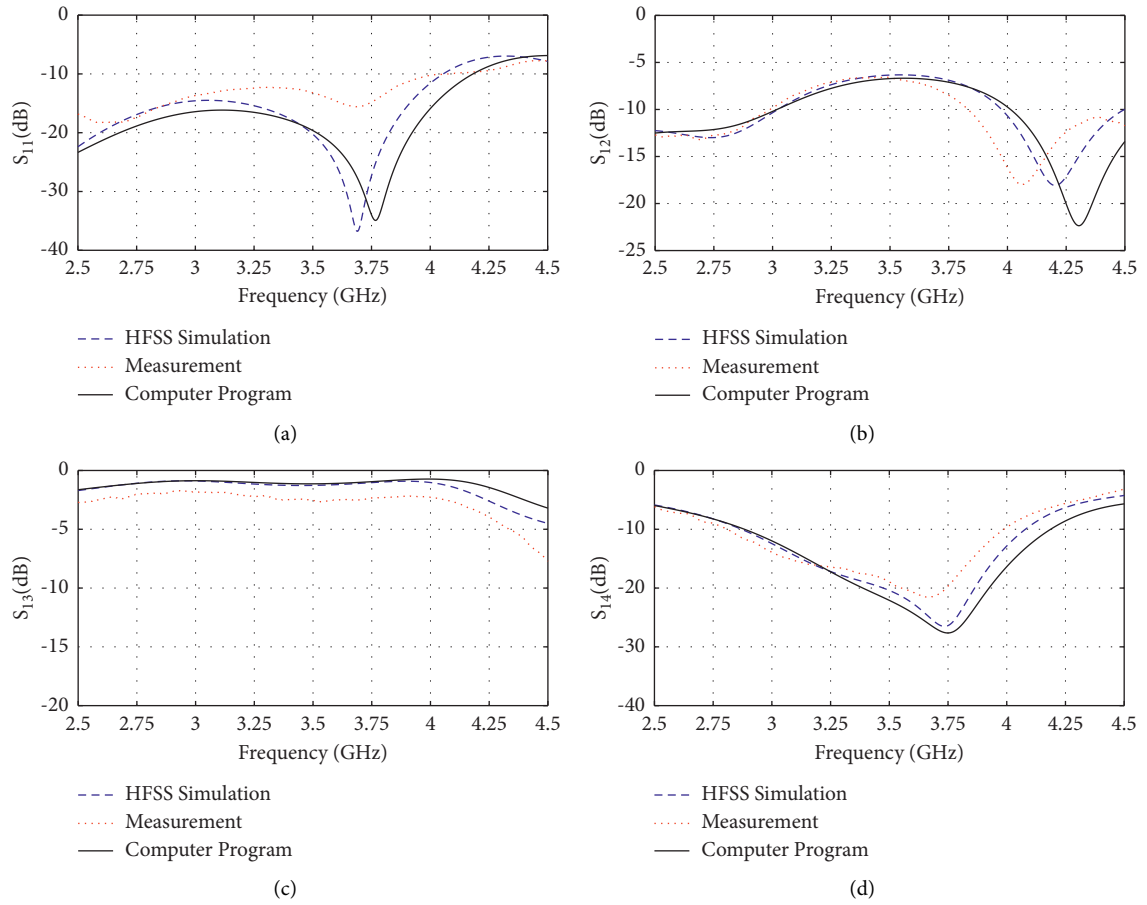


Figure 13: Frequency response of 6 dB ATRD coupler. (a) Reflection Loss; (b) Coupling coefficient; (c) Through coefficient; (d) Isolation Coefficient.

program optimization on personal computer Core i5 @1.8 GHz, takes **7.035879 seconds**, but HFSS software takes **540 seconds** for this process. Therefore, computer program is about 76 times faster than the full-wave simulation software, in this example. A prototype model of this ATRD coupler is fabricated and shown in Figure 12. The metal traces are gold-plated and the standard capacitor with foot prints of 0603, 0402 (in inch) are used.

Its frequency response obtained by the equivalent circuit (computer program), full-wave simulation (HFSS) and measurements are reported in Figure 13 for comparison. Its scattering parameters $S_{11}, S_{12}, S_{13}$ and $S_{14}$ are drawn in Figures 13(a)–13(d). Same as example 3.1, the results from the MLS design and HFSS software simulation are in good agreement. The measurement results are also included in the drawings of these figures which are all in good agreement. However, the discrepancies among the results of HFSS simulation and computer program and measurement data are due to imperfect soldering, losses in capacitors, manufacture imprecision of spacings among coupled tracks.

Based on the measurement results, in the designed frequency band $|S_{11}|$ dB $< -12$ dB with the minimum point of -15.5 dB at 3.7 GHz, the coupling value $|S_{12}|$ dB is about $-7.3 \pm 0.6$ dB, the power delivered to through port $|S_{13}|$ dB is about $-2.1 \pm 0.3$, and the isolation $|S_{14}|$ at isolated port is less than $-15.5$ dB with

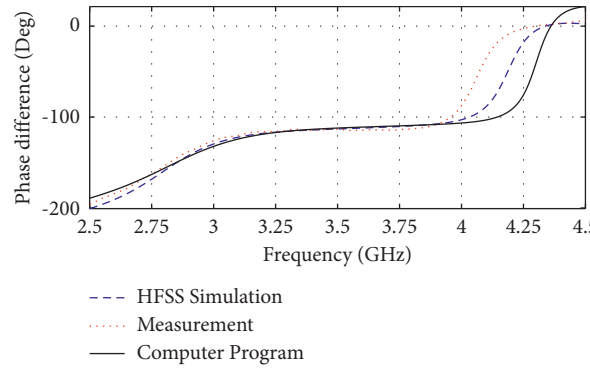


Figure 14: Phase difference between through and coupled ports of 6 dB ATRD coupler.

the best achievement of $-21.4$ dB at 3.7 GHz. The phase difference between coupled and through port are shown in Figure 14. Results of computer program and HFSS simulation and measurement have good agreement. The measurement phase difference is $114 \pm 15^{\circ}$ in 3.3–3.7 GHz frequency range.

*3.3. Example 3: Design 10 dB Asymmetric Transdirectional Coupler.* A 10 dB ATRD coupler is designed with different port impedances of 50, 60, 75 and 50 ohms at ports 1,2,3 and

Table 7: Values of (9) for design 10 dB ATRD coupler has been described in Example 3.

| $W_1$ | $W_2$ | $W_3$ | $W_4$ | $W_5$ | $W_6$ | $W_7$ | $W_8$ | $W_9$ | $W_{10}$ | $W_{11}$ | $C$ $(dB)$ | $T$ $(dB)$ | $L_C^U$ $(dB)$ | $L_C^D$ $(dB)$ | $L_T^U$ $(dB)$ | $L_T^D$ $(dB)$ |
|---|---|---|---|---|---|---|---|---|---|---|---|---|---|---|---|---|
| 1 | 1 | 1 | 1 | 1 | 4 | 4 | 2 | 2 | 2 | 2 | −10 | −0.45 | −13 | −13 | −3.5 | −3.5 |

Table 8: Dimension and capacitor value for design 10 dB ATRD coupler has been described in Example 3.

| Section | $W_U(i)$ $(mm)$ | $W_D(i)$ $(mm)$ | $S(i)$ $(mm)$ | $L(i)$ $(mm)$ | $C(i)$ $(pF)$ |
|---|---|---|---|---|---|
| 1 | 1.3 < **1.58** < 2 | 0.9 < **1.08** < 1.3 | 0.2 < **1.9** < 2 | 0.5 < **2.99** < 5 | 0.2 ≤ **0.2** < 4 |
| 2 | 0.2 < **1.76** < 3 | 0.2 < **2.5** < 3 | 0.2 < **1.38** <2 | 0.5 < **3.85** < 5 | 0.2 ≤ **0.2** < 4 |
| 3 | 0.2 < **1.88** < 3 | 0.2 < **1.41** < 3 | 0.2 < **1.25** < 2 | 0.5 < **1.04** < 5 | 0.2 < **0.2** < 4 |
| 4 | 0.2 < **0.69** < 3 | 0.2 < **1.03** < 3 | 0.2 < **1.9** < 2 | 0.5 < **2.74** < 5 | 0.2 ≤ **0.5** < 4 |
| 5 | 0.2 < **2.22** < 3 | 0.2 < **2.69** < 3 | 0.2 < **0.87** < 2 | 0.5 < **2.7** < 5 | 0.2 ≤ **0.2** < 4 |
| 6 | 0.2 < **0.57** < 3 | 0.2 < **1.03** < 3 | 0.2 < **1.95** < 2 | 0.5 < **1.8** < 5 | 0.2 ≤ **0.2** < 4 |
| 7 | 0.2 < **0.59** < 3 | 0.2 < **0.51** < 3 | 0.2 < **1.97** < 2 | 0.5 < **1.17** < 5 | 0.2 ≤ **0.5** < 4 |
| 8 | 0.2 < **0.87** < 3 | 0.2 < **0.59** < 3 | 0.2 < **1.7** < 2 | 0.5 < **1.09** < 5 | 0.2 ≤ **0.2** < 4 |
| 9 | 0.2 < **0.56** < 3 | 0.2 < **0.62** < 3 | 0.2 < **1.91** < 2 | 0.5 < **1.69** < 5 | 0.2 ≤ **0.2** < 4 |
| 10 | 1.3 < **1.57** < 2 | 0.5 < **0.74** < 1 | 0.2 < **1.31** < 2 | 0.5 < **1.09** < 5 | 0.2 ≤ **0.5** < 4 |

Table 9: Dimension of feed lines for design 10 dB ATRD coupler has been described in Example 3.

| $L_{f1}$ $(mm)$ | $L_{f2}$ $(mm)$ | $L_{f3}$ $(mm)$ | $L_{f4}$ $(mm)$ |
|---|---|---|---|
| 5.15 | 5.15 | 5.8 | 5.45 |

4, respectively. It has been designed on 3.1–3.9 GHz, which allocated to the WI-MAX frequency band. It consists of 10 cascaded sections and designed on the Rogers 4003 substrate with thickness = 0.8mm. The parameters of (8) are set as in Table 7, to design 10 dB ATRD coupler, C sets to −10 dB, $T$ sets to -0.15 dB and out of band attenuation sets to 3 dB lower than C and $T$ values, for coupled and through ports. The final values of dimensions and capacitors as well as their variation range in optimization process are shown in Table 8. The dimensions of terminal lines are given in Table 9. Every loop of computer program optimization on personal computer Core i5 @1.8 GHz, takes **7.195208 seconds**, but HFSS software takes **498 seconds** for this process. Therefore, computer program is about 70 times faster than the full-wave simulation software, in this example.

A prototype model of this ATRD coupler is fabricated and Its photograph is shown in Figure 15. The metallic tracks are gold-plated for improved performance. Its frequency responses obtained by the equivalent circuit (computer program), full-wave simulation (HFSS) and measurements are reported in the figures for comparison. Its frequency response for $S_{11}$, $S_{12}$, $S_{13}$ and isolated port $S_{14}$ are shown in Figures 16, 16(a)–16(d), respectively.

In this example, there is a little shift between the scattering parameters of circuit model and HFSS simulation. However, the frequency responses in the designed frequency band, have acceptable behavior. This frequency shift is due to several causes, such as tolerances of section widths which have been ignored in equivalent circuit model for simplicity. On the other hand the HFSS simulation results and measurement results are in good agreement. However, a frequency shift in Figure 16(d) and also a difference between

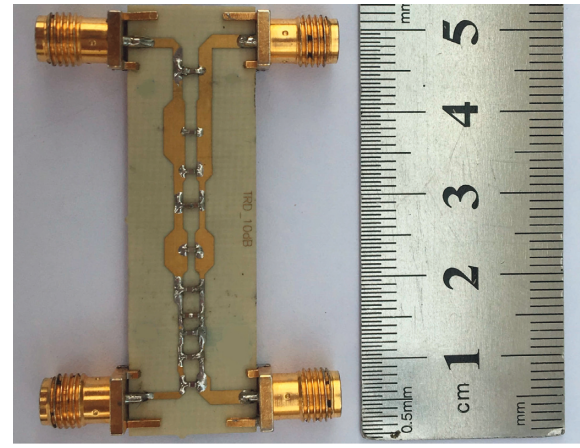


Figure 15: Fabricated 10 dB ATRD coupler of Example 3.

HFSS simulation and measurement in Figures 16(b), 16(c) may be due to imperfect soldering, loss in capacitors and imprecision of spacings among coupled lines, and unadjusted of spacings and standard capacitors sizes.

Based on measurement results in the designed frequency range, $|S_{11}|$ dB < − 10.5 dB with minimum point -19.7 dB at 3.67 GHz, coupling value $|S_{12}|$ dB is about −11.9 ± 0.4 dB and power delivered to through port $|S_{13}|$ dB is about −1.2 ± 0.6 dB and isolation $|S_{14}|$ dB < − 11.5 dB dB with minimum −79.2 dB at 3.52 GHz. The phase difference between coupled and through port are shown in Figure 17. Results of HFSS simulation and measurement have good agreement in designed frequency range. Due to the computer program do not cover all of the properties that effect on results as full-wave simulation software and measurement, the result of computer program have a bit difference with others.

In [8] using the CPW lines with DGS, a 10 dB TRD coupler has been designed. It is claimed that the realization of such weak TRD couplers on microstrip technology is impossible. However, a 10 dB ATRD coupler is designed in our paper with asymmetrical coupled lines.

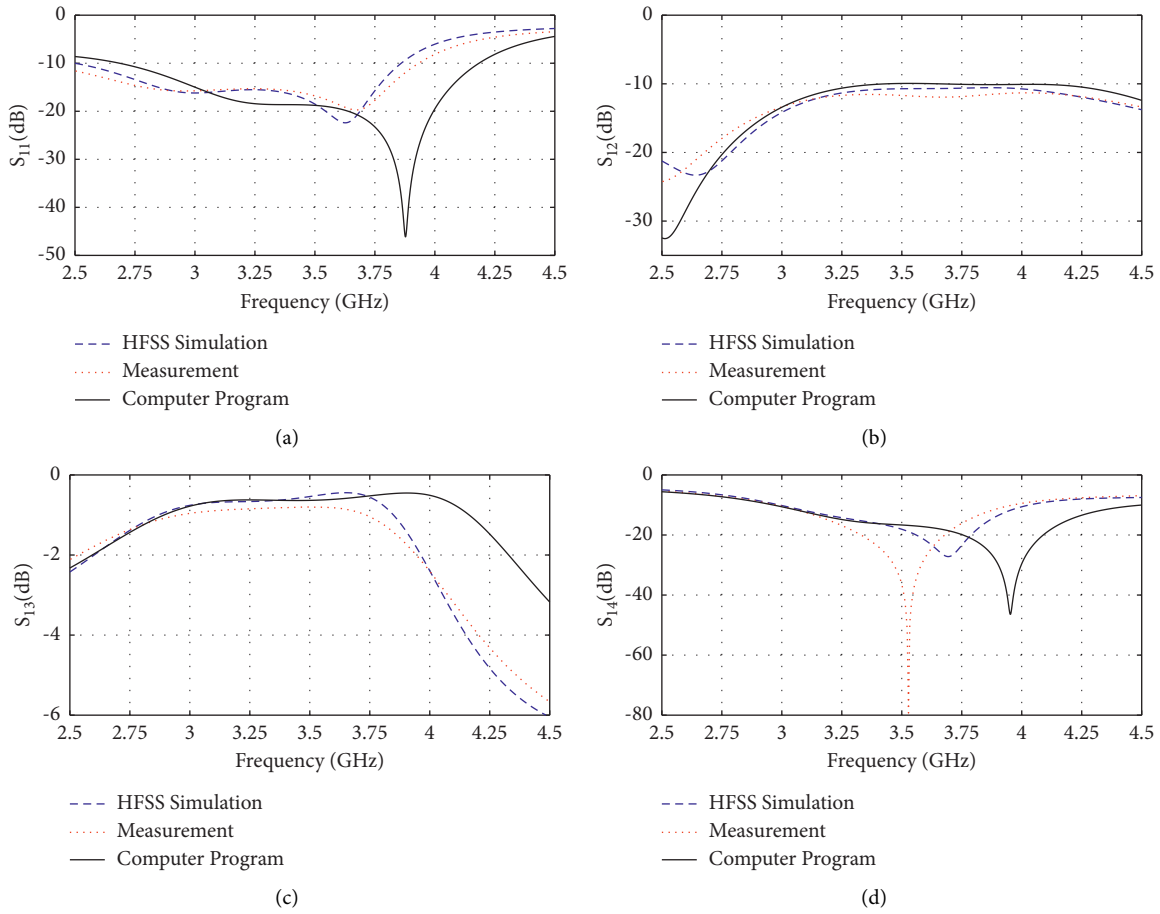


Figure 16: Frequency response of 10 dB ATRD coupler. (a) Reflection Loss (b) Coupling coefficient; (c) Through coefficient.; (d) Isolation coefficient.

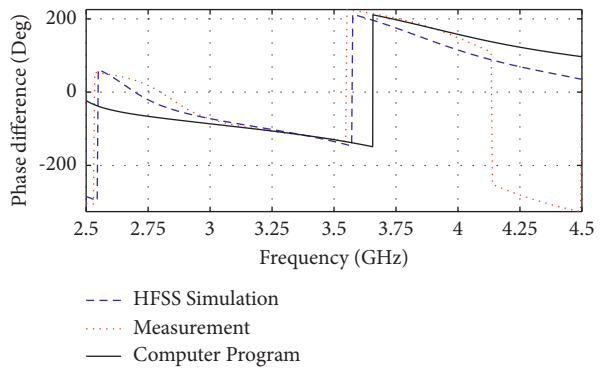


Figure 17: Phase difference between through and coupled ports of 10 dB ATRD coupler.

Table 10: Compression between TRD coupler in other papers and this study 10 dB ATRD coupler.

| Reference | Isolation > 20 dB | Through | Coupling | Return loss >rbin 15 dB | Technology | Structure |
|---|---|---|---|---|---|---|
| [8] | 1.421–1.520 GHz (6.3%) | 0.68 ± 0.2 dB | 10.8 ± 0.4 dB | 1.36–1.66 GHz (19.8%) | DGS CPWs | Symmetrical |
| [6] | 3.31–3.93 GHz (17.13%) | 2.18 ± 0.18 dB | 2.5 ± 0.5 dB | 3.05–4.1 GHz (29.3%) | Single layer PCB | Symmetrical |
| [7] | 1.5–1.69 GHz (11.91%) | 3.47 ± 0.33 dB | 3.18 ± 0.37 dB | 1.42–1.82 GHz (24.6%) | Single layer PCB | Symmetrical |
| This study | 3.32–3.68 GHz (10.2%) | 0.86 ± 0.03 dB | −11.7 ± 0.2 dB | 2.7–3.8 GHz (33.8%) | Single layer PCB | Asymmetrical |

In Table 10, the comparison of this study 10 dB ATRD coupler with other TRD couplers in the literature, has been reported. The through and coupled output power values exhibit on isolation greater than 20 dB. According to Table 10, in comparison to [8], this paper ATRD coupler bandwidth has been improved. Also, the through and coupled port power characteristics of this study ATRD are flatter than the available works in the literature. Note that this paper ATRD asymmetrical coupler uses only a single layer PCB technology, which has a simple realization, compared to other conventional symmetrical TRD couplers.

## 4. Conclusion

The goal of this paper is design general weak or strong transdirectional coupler with arbitrary coupling coefficient and arbitrary port impedances. The asymmetrical coupled lines are adopted and analyzed by the $c$ and $\pi$ modes, contrary to the even- and odd-mode analysis for the symmetrical coupled lines. The outcome, is the method of design any weak or strong ATRD coupler with port impedance matching and any desired operating frequency and bandwidth. An equivalent circuit model for the ATRD coupler is described, then the scattering parameters of the four port network (ATRD coupler) are derived by obtaining its impedance matrix and then its transmission matrix. The transformations between the impedance, transmission and scattering matrices of a cascade of four port networks are presented in detail. Finally, optimization and design based on the method of least squares (MLS) is developed based on the equivalent circuit of the ATRD coupler. The constructed error function is minimized to determine the geometrical dimensions of ATRD coupler for the realization of specified coupling coefficient and impedance matching at its ports for any specified frequency bandwidth. The performance of the designed ATRD coupler is finally evaluated by full-wave computer simulation software and measurement. As a proof of concept, two prototype models of ATRD couplers are designed and fabricated according to the specifications. Observe that the proposed MLS design algorithm based on the equivalent circuit of a ATRD coupler takes a relatively short CPU time for the determination its geometrical dimensions compared to the effort and CPU time required by a full-wave simulation software. The examples presented in this paper, report the average CPU times of a single run of proposed algorithm computer program and the full-wave simulation software, which this time for computer program is about 80 times faster than full-wave simulation software.

## Data Availability

The computer program data used to support the findings of this study are available from the corresponding author upon request.

## Conflicts of Interest

The authors declare that they have no conflicts of interest.

## References

[1] H. Oraizi and G. R. G. Ghadim, "Optimum design of broadband multisection coupled-line couplers with arbitrary coupling and impedance matching," *IEICE - Transactions on Communications*, vol. 86, no. 9, pp. 2709–2719, 2003.

[2] R. Levy, "Tables for asymmetric multi-element coupled-transmission-line directional couplers," *IEEE Transactions on Microwave Theory and Techniques*, vol. 12, no. 3, pp. 275–279, 1964.

[3] E. G. Cristal and L. Young, "Theory and tables of optimum symmetrical TEM-mode coupled-transmission-line directional couplers," *IEEE Transactions on Microwave Theory and Techniques*, vol. 13, no. 5, pp. 544–558, 1965.

[4] D. W. Kammler, "The design of discrete N-section and continuously tapered symmetrical microwave TEM directional couplers," *IEEE Transactions on Microwave Theory and Techniques*, vol. 17, no. 8, pp. 577–590, 1969.

[5] M. Bona, L. Manholm, J. P. Starski, and B. Svensson, "Low-loss compact Butler matrix for a microstrip antenna," *IEEE Transactions on Microwave Theory and Techniques*, vol. 50, no. 9, pp. 2069–2075, 2002.

[6] J.-C Ching-Ian Shie, S.-C. Sheng-Chun Chou, and Yi-C. Yi-Chyun Chiang, "Transdirectional coupled-line couplers implemented by periodical shunt capacitors," *IEEE Transactions on Microwave Theory and Techniques*, vol. 57, no. 12, pp. 2981–2988, 2009.

[7] H Liu, S.-J Fang, Z Wang, and Y Zhou, "Miniaturization OF TRANS-directional coupled line couplers using series inductors," *Progress In Electromagnetics Research C*, vol. 46, pp. 171–177, 2014.

[8] H. M. Liu, Z. B. Wang, and S. J. Fang, "Trans-directional coupler with capacitor-shunted ground-defected coupled CPWs and inductor-loaded ACPWs for weak coupling applications," *Journal of Electromagnetic Waves and Applications*, vol. 27, no. 1, pp. 104–116, 2013.

[9] H. Liu, S. Fang, and Z. Wang, "Trans-directional coupler with adjustable coupling coefficients and reconfigurable responses," *IET Microwaves, Antennas & Propagation*, vol. 11, no. 10, pp. 1340–1346, 2017.

[10] T. Emery, Y. Chin, H. Lee, and V. K. Tripathi, "Analysis and design of ideal non symmetrical coupled microstrip directional couplers," in *Proceedings of the IEEE MTT-S International Microwave Symposium Digest*, Long Beach, CA, USA, June 1989.

[11] S. Kal, D. Bhattacharya, and N. B. Chakraborti, "Normal-mode parameters of microstrip coupled lines of unequal width (short paper)," *IEEE Transactions on Microwave Theory and Techniques*, vol. 32, no. 2, pp. 198–200, 1984.

[12] V. K. Tripathi and Y. K. Chin, "Analysis of the general nonsymmetrical directional coupler with arbitrary terminations," *IEE Proceedings H Microwaves, Optics and Antennas*, vol. 129, no. 6, p. 360, 1982.

[13] V. K. Tripathi and C. L. Chang, "Quasi-TEM parameters of non-symmetrical coupled microstrip lines†," *International Journal of Electronics*, vol. 45, no. 2, pp. 215–223, 1978.

[14] E. G. Cristal, "Coupled-transmission-line directional couplers with coupled lines of unequal characteristic impedances," *IEEE Transactions on Microwave Theory and Techniques*, vol. 14, no. 7, pp. 337–346, 1966.

[15] V. K. Tripathi, "Asymmetric coupled transmission lines in an inhomogeneous medium," *IEEE Transactions on Microwave Theory and Techniques*, vol. 23, no. 9, pp. 734–739, 1975.

[16] K. Wincza and S. Gruszczynski, "Asymmetric coupled-line directional couplers as impedance transformers in balanced and $n$-Way power amplifiers," *IEEE Transactions on Microwave Theory and Techniques*, vol. 59, no. 7, pp. 1803–1810, 2011.

[17] H. Oraizi and A.-R. Sharifi, "Design and optimization of broadband asymmetrical multisection wilkinson power divider," *IEEE Transactions on Microwave Theory and Techniques*, vol. 54, no. 5, pp. 2220–2231, 2006.

[18] K. Kurokawa, "Power waves and the scattering matrix," *IEEE Transactions on Microwave Theory and Techniques*, vol. 13, no. 2, pp. 194–202, 1965.